

## Supporting Information for

### Minimally disruptive optical control of protein tyrosine phosphatase 1B

Akarawin Hongdusit<sup>a</sup>, Peter H. Zwart<sup>b</sup>, Banumathi Sankaran<sup>b</sup>, and Jerome M. Fox<sup>a\*</sup>

<sup>a</sup>Department of Chemical and Biological Engineering, University of Colorado Boulder,  
3415 Colorado Avenue, Boulder, CO, 80303

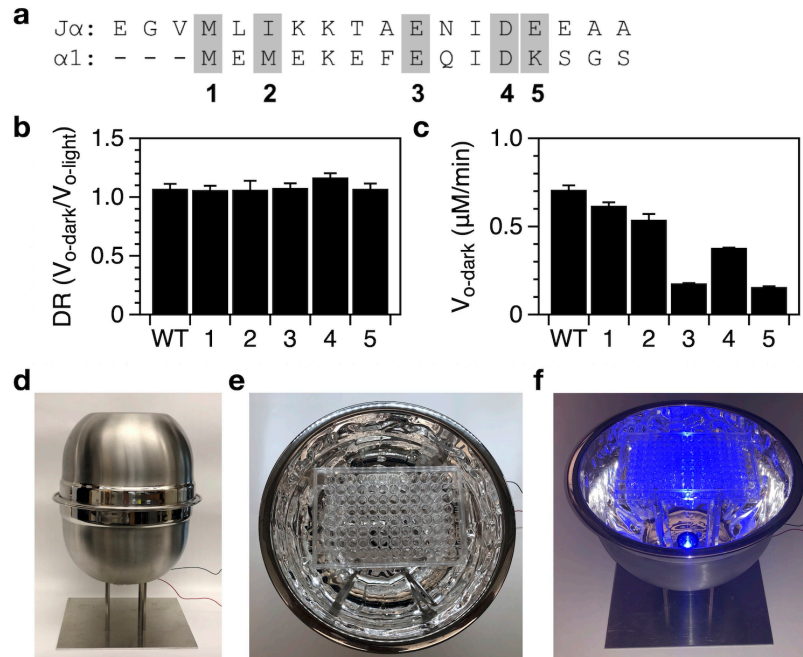
<sup>b</sup>Molecular Biophysics and Integrated Bioimaging, Lawrence Berkeley National Laboratory, 1  
Cyclotron Road, Berkeley, CA, 94720

\*To whom correspondence should be addressed. E-mail: [jerome.fox@colorado.edu](mailto:jerome.fox@colorado.edu)

Supplementary Notes 1-2.....	S2
Supplementary Figures 1-12.....	S4
Supplementary Tables 1-10.....	S17
SI References.....	S31

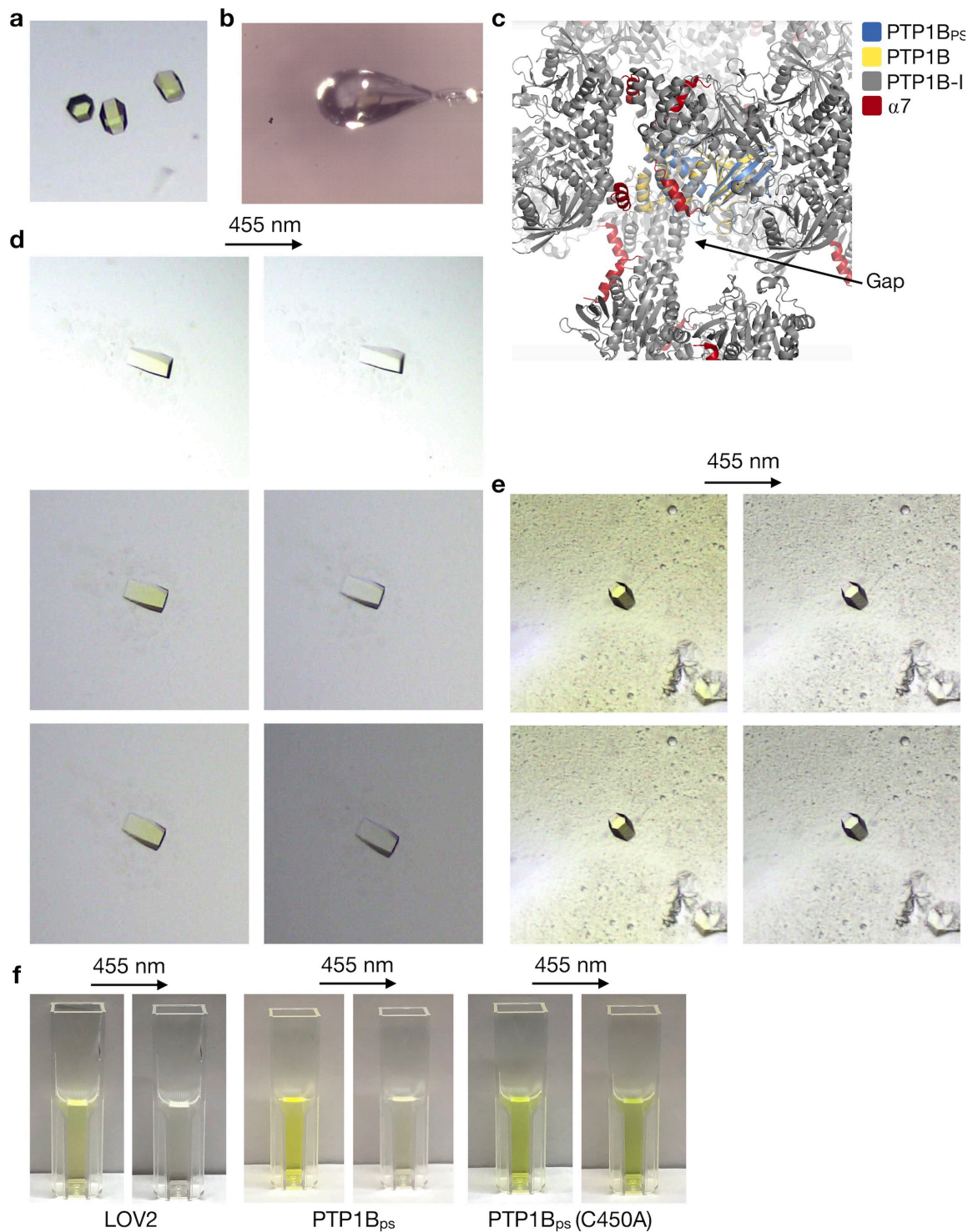
**Supplementary Note 1. Analysis of the crystal structure of PTP1B<sub>PS</sub>.** We used X-ray crystallography to examine the structural integrity of PTP1B within the PTP1B<sub>PS</sub> chimera (Table 1). Crystals of PTP1B<sub>PS</sub> exhibited three surprising features (Fig. 1d and Supplementary Figs. 2 and 3): (i) Their unit cell and space group were indistinguishable from those of previously collected crystals of PTP1B and PTP1B-ligand complexes. (ii) They permitted resolution of PTP1B, but not LOV2. (iii) They showed PTP1B with a wild-type conformation (i.e., the root-mean-square deviation of aligned atoms between the catalytic domains of PTP1B<sub>PS</sub> and wild-type PTP1B was 0.30 Å). These features, considered alone, might indicate that LOV2 is absent from our crystals; four additional crystallographic attributes, however, contradict this interpretation: (i) Our crystals were yellow, a color derived from LOV2 (a consequence of its FMN cofactor<sup>1,2</sup>; Supplementary Figures 2a and 2b). (ii) When exposed to 455-nm light, the crystals turned clear, an indication that LOV2 remains capable of forming a cysteine adduct with FMN (Supplementary Figures 2d and 2e). We note: Solutions of PTP1B<sub>PS</sub>(C450M), which cannot form the cysteine adduct, do not photoswitch (Supplementary Figure 2f). (iii) The unit cell had a gap near the  $\alpha 7$  helix, the attachment point of LOV2 (Supplementary Figure 2c). (iv) Previously examined apo structures of PTP1B in which the  $\alpha 7$  helix is disordered possess the same unit cell and space group as our crystals.<sup>3</sup> These features, taken together, suggest that disorder in the  $\alpha 7$  helix of PTP1B causes variability in the orientation of LOV2 within the crystal lattice. Broadly, PTP1B crystallizes with the same space group, unit cell, and conformation in the presence and absence of LOV2 and, thus, appears to be structurally unperturbed (to the extent detectable with X-ray crystallography) by this light-sensitive fusion partner.

**Supplementary Note 2. Quantitative analysis of insulin receptor phosphorylation with an enzyme-linked immunosorbent assay (ELISA).** The signals afforded by enzyme-linked immunosorbent assays (ELISAs) are notoriously nonlinear<sup>4,5</sup>. To quantify sample-to-sample differences in concentrations of phosphorylated insulin receptor—an analyte that lacks a commercially available standard—we carried out the following steps: (i) We fit a dilution curve (i.e., a plot of assay signal vs. dilution factor) for each sample to a four-parameter logistic equation (Supplementary Table 9). (ii) We used the dilution curve of each sample of interest to estimate the difference in analyte concentration between that “reference” sample and a second sample. For example, on a particular dilution curve (e.g., the curve for HEK293T/17 cells exposed to 10 nM of insulin), the signal afforded by a dilution factor of 1 corresponds to the undiluted analyte concentration in the cell lysate, and the signal afforded by a dilution factor of 0.5 corresponds to one-half of that concentration. By solving for the dilution factor associated with the signal of a second undiluted sample (e.g., PTP1B<sub>PS\*\*</sub>-expressing HEK293T/17 cells exposed to 455 nm light), we estimated the fold-difference in analyte concentration between the two samples (e.g., a dilution factor of 0.25 indicates that the second sample has four-fold less phosphorylated insulin receptor than the first sample). (iii) To check the consistency of our analysis, we used the dilution curve for the second sample to estimate, once again, the difference in analyte concentration between the two samples. In all cases, the two estimates—each based on a separate dilution curve—differed by less than 40%. (iv) We calculated the average and standard deviation of the two estimates (Supplementary Table 10 and Supplementary Figure 12). The results of our analysis suggest that transient illumination of PTP1B<sub>PS\*\*</sub> enables a >20-fold change in the concentration of phosphorylated insulin receptor within the cell.



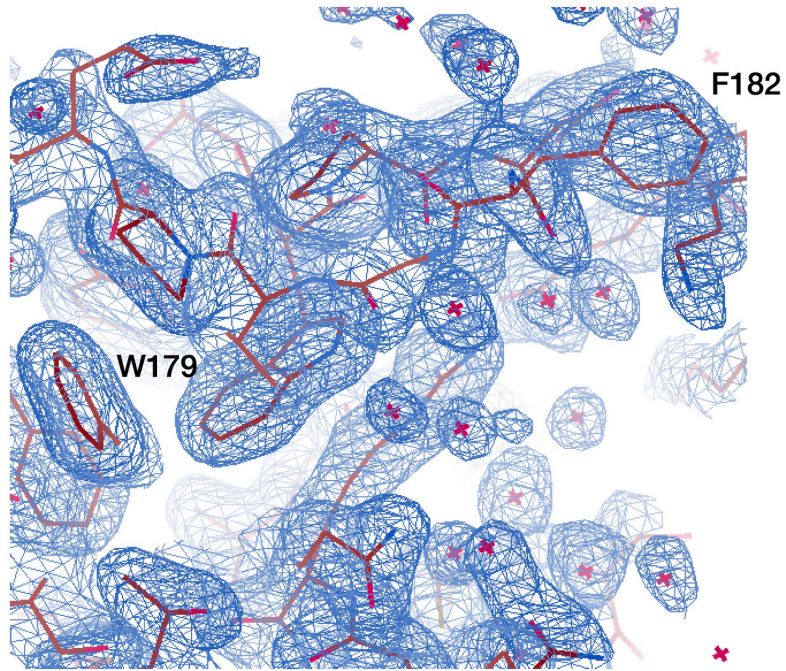
**Supplementary Figure 1 | Analysis of LOV2-PTP1B chimeras.** **a**, We complemented our initial set of chimeras (Fig. 1b) by constructing a second set in which the C-terminal Jα helix of LOV2 is fused to the N-terminus of PTP1B at homologous crossover points. **b-c**, Assays of these chimeras on 4MUP indicate that their catalytic activities are **(b)** light-insensitive and **(c)** significantly reduced (relative to wild-type). The plotted data depict the mean and SE for  $n \geq 6$  independent experiments. **d**, The light chamber used for *in vitro* reactions. We coated two stainless steel mixing bowls (Crate and Barrel) with reflective foil and assembled them into a reflective chamber. To the bottom half of this chamber, we added both (i) a 455 nm LED light (SLS-0301-C, Mightex Systems), fed through a hole, and (ii) four steel rods. **e**, The bottom half of the chamber loaded with a 96-well plate. **f**, An image showing the blue light at full power (~450 mW). Source data are provided as a Source Data file.



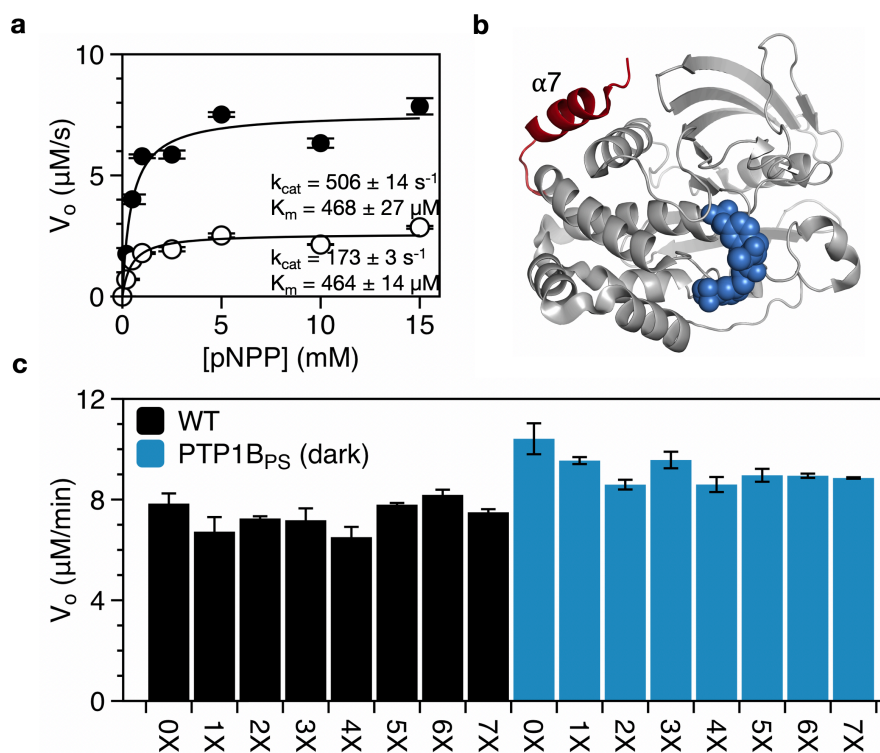


**Supplementary Figure 2 | Crystals of PTP1B-LOV2 chimeras.** **a**, Crystals of PTP1B-LOV2 chimeras appeared yellow (or yellow green), an indication that they contained LOV2. **b**, The crystal of PTP1B<sub>ps</sub> used to collect X-ray diffraction data; close inspection reveals a yellow tinge.

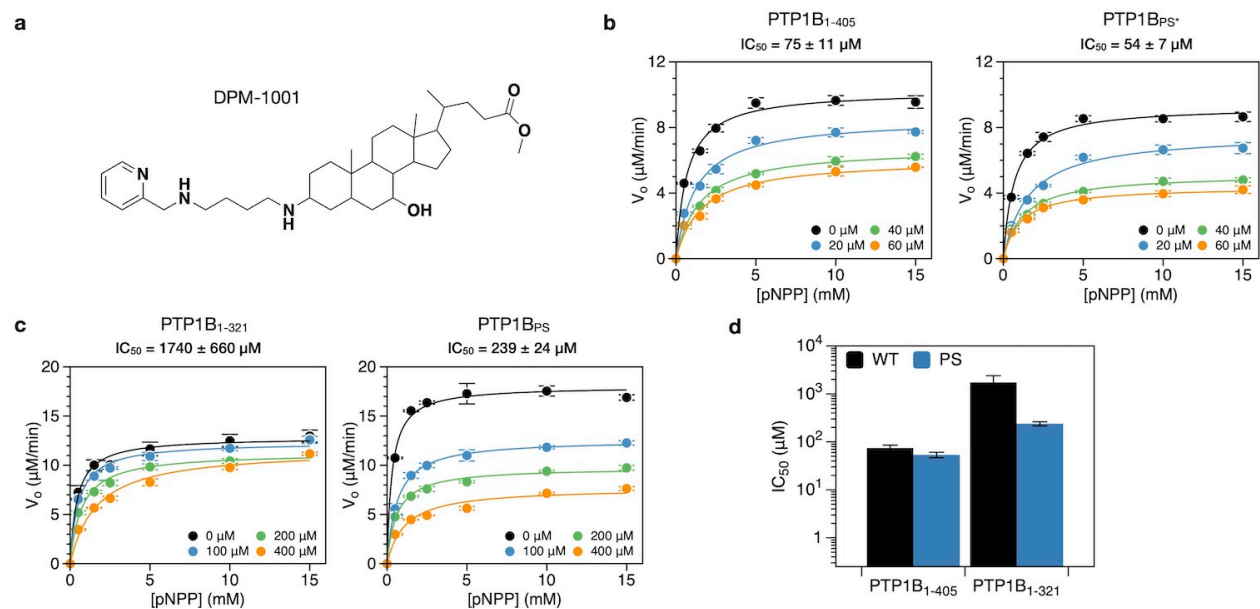
**c**, Aligned catalytic domains of PTP1B in three structures: photoswitchable (6ntp), apo (3a5j), and competitively inhibited (2f71). Neighboring asymmetric units from the crystal of the competitively inhibited structure ( $\alpha$ 7 helix in red) surround the aligned structures (30-Å cutoff). A gap exists near the  $\alpha$ 7 helix, the attachment point for LOV2. We note: 6ntp and 2f71 have the same space group (P3<sub>1</sub>21) and unit cell dimensions. **d-e**, When exposed to 455-nm light (10-seconds, ~450 mW), crystals of PTP1B<sub>PS</sub> switched from yellow (oxidized FMN) to clear (reduced FMN); incubation in the dark (5 minutes) restored their yellow color and enabled repeated photoswitching (1x, 2x, and 3x). **f**, When exposed to 455-nm light (10 seconds), solutions containing only LOV2 or PTP1B<sub>PS</sub> transitioned from yellow to clear, while a solution of PTP1B<sub>PS</sub>(C450M) remained yellow.



**Supplementary Figure 3 | Crystallographic analysis of PTP1B<sub>PS</sub>.** An electron density map shows the WPD loop of PTP1B in the crystal structure of PTP1B<sub>PS</sub> (FWT 1.02  $\sigma$ ); the loop is in the open position. As discussed above, the LOV2 domain of PTP1B<sub>PS</sub> was unresolvable.

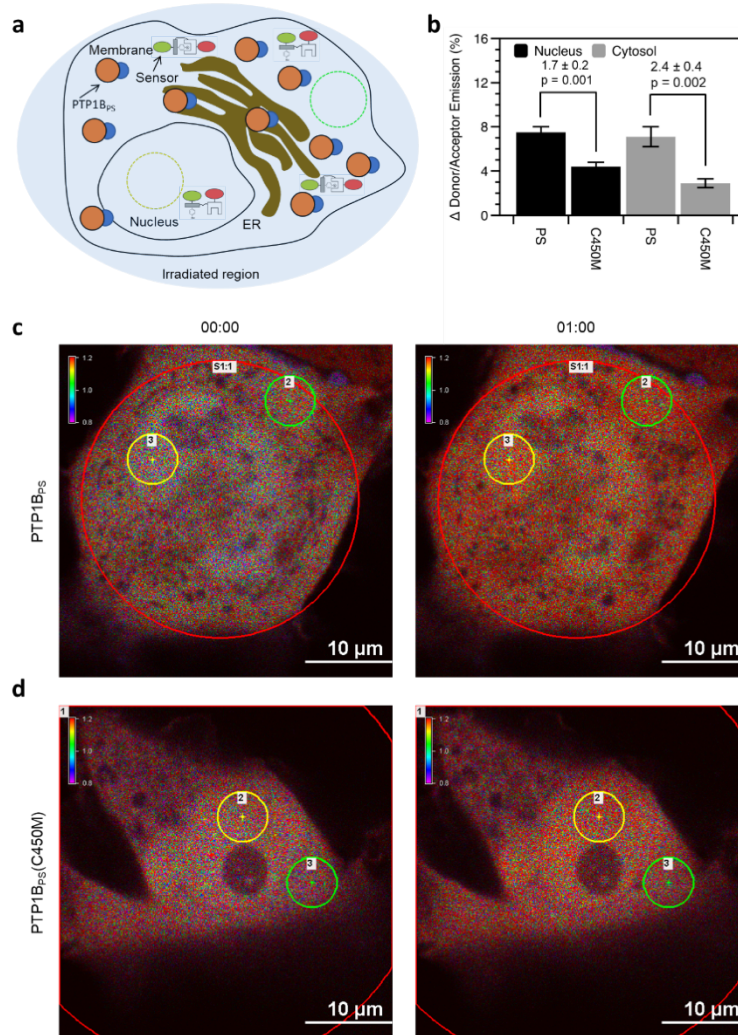


**Supplementary Figure 4 | Analysis of activity on p-nitrophenyl phosphate (pNPP).** **a**, Initial rates of pNPP hydrolysis by PTP1B<sub>321</sub> (black) and PTP1B<sub>281</sub> (white); lines that denote nonlinear least-squares fits to a Michaelis-Menten model. A difference in  $k_{cat}$ 's of  $2.92 \pm 0.10$  suggests that the DR of PTP1B<sub>PS</sub> ( $2.50 \pm 0.04$  on the same substrate) is 85% of the maximum achievable value for a photoswitch that exploits changes in the conformation of the  $\alpha 7$  helix. **b**, A crystal structure of PTP1B (pdb entry 2f71) bound to a competitive inhibitor (blue spheres). Residues 282-298 (red) are missing in PTP1B<sub>281</sub>. **c**, Initial rates of pNPP hydrolysis by PTP1B<sub>PS</sub> after repeated exposure with 455 nm light (i.e., for each test, we irradiated PTP1B<sub>PS</sub> with blue light for 10 seconds and waited 5 min after irradiation to perform kinetic assays). PTP1B<sub>PS</sub> maintains its dark-state activity after multiple cycles of exposure. For **a** and **c**, error bars denote SE for  $n \geq 3$  independent reactions. Source data are provided as a Source Data file.

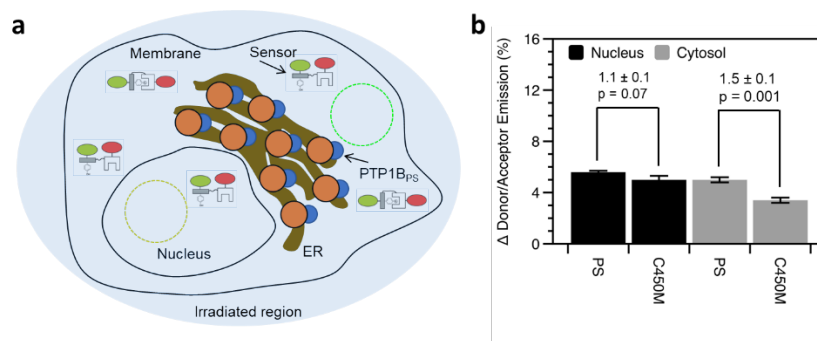


**Supplementary Figure 5 | Analysis of full-length constructs. a**, The molecular structure of DPM-1001, an inhibitor that binds preferentially to the disordered C-terminus of PTP1B. **b**, Inhibition of PTP1B<sub>1-405</sub> and PTP1B<sub>PS\*</sub> by DPM-1001. **c**, Inhibition of PTP1B<sub>1-321</sub> and PTP1B<sub>PS</sub> by DPM-1001. **d**, A comparison of IC<sub>50</sub>'s for DPM-1001 on wild-type variants (PTP1B<sub>1-321</sub> and PTP1B<sub>1-405</sub>) and photoswitchable constructs (PTP1B<sub>PS</sub> and PTP1B<sub>PS\*</sub>); LOV2 alters the IC<sub>50</sub> of the full-length PTP1B by 30%. For all figures, error bars denote SE for  $n \geq 6$  independent reactions. Source data are provided as a Source Data file.

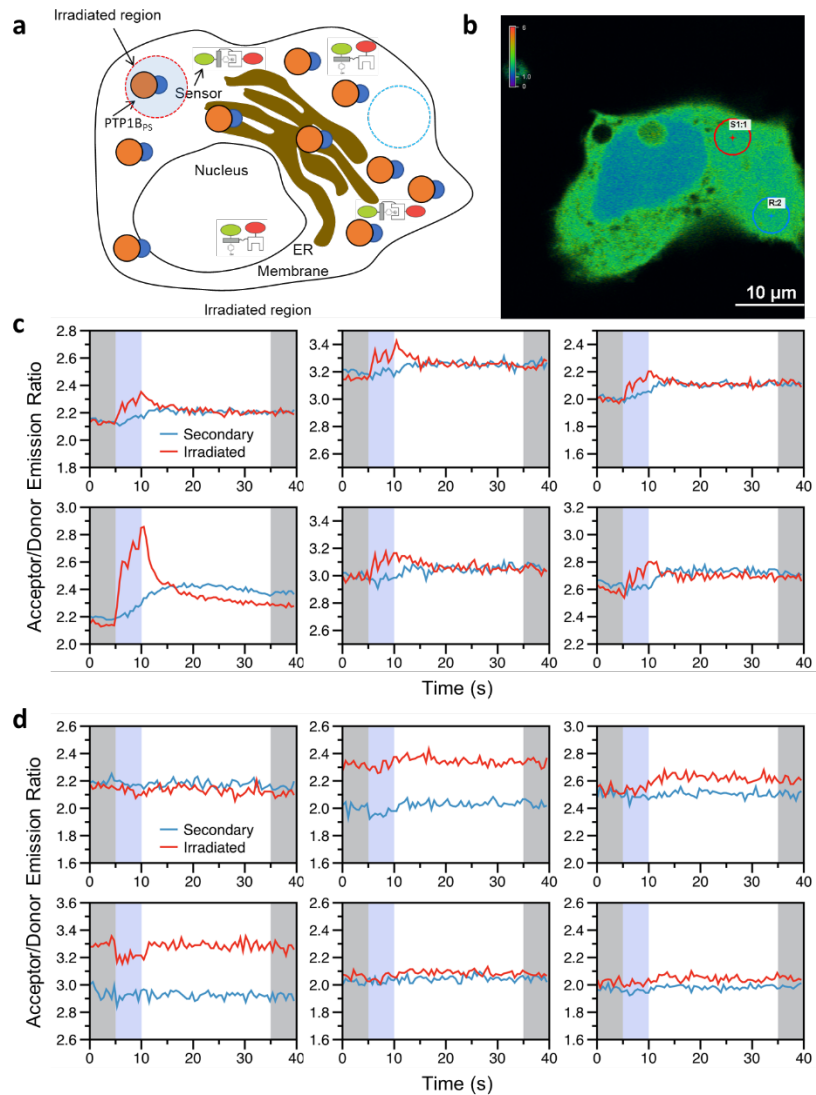




**Supplementary Figure 6 | Whole-cell irradiation of PTP1B<sub>PS</sub>.** **a**, A COS-7 cell expressing both PTP1B<sub>PS</sub> and a biosensor is irradiated with blue light (457 nm). Circles depict the irradiated region (light blue oval), a nuclear region (yellow circle, d = 5 μm), and a cytosolic region (green circle, d = 5 μm). **b**, The percent change in donor/acceptor emission ratio over 1 min in nuclear and cytosolic regions. Each condition includes the interquartile average and SE for n = 11 biological replicates. **c**, Images of a COS-7 cell expressing both PTP1B<sub>PS</sub> and a biosensor at (left) 0 min after irradiation with blue light and (right) 1 min after irradiation. **d**, Images of a COS-7 cell expressing both PTP1B<sub>PS</sub>(C450M) and a biosensor at (left) 0 min after irradiation with blue light and (right) 1 min after irradiation. Source data are provided as a Source Data file.

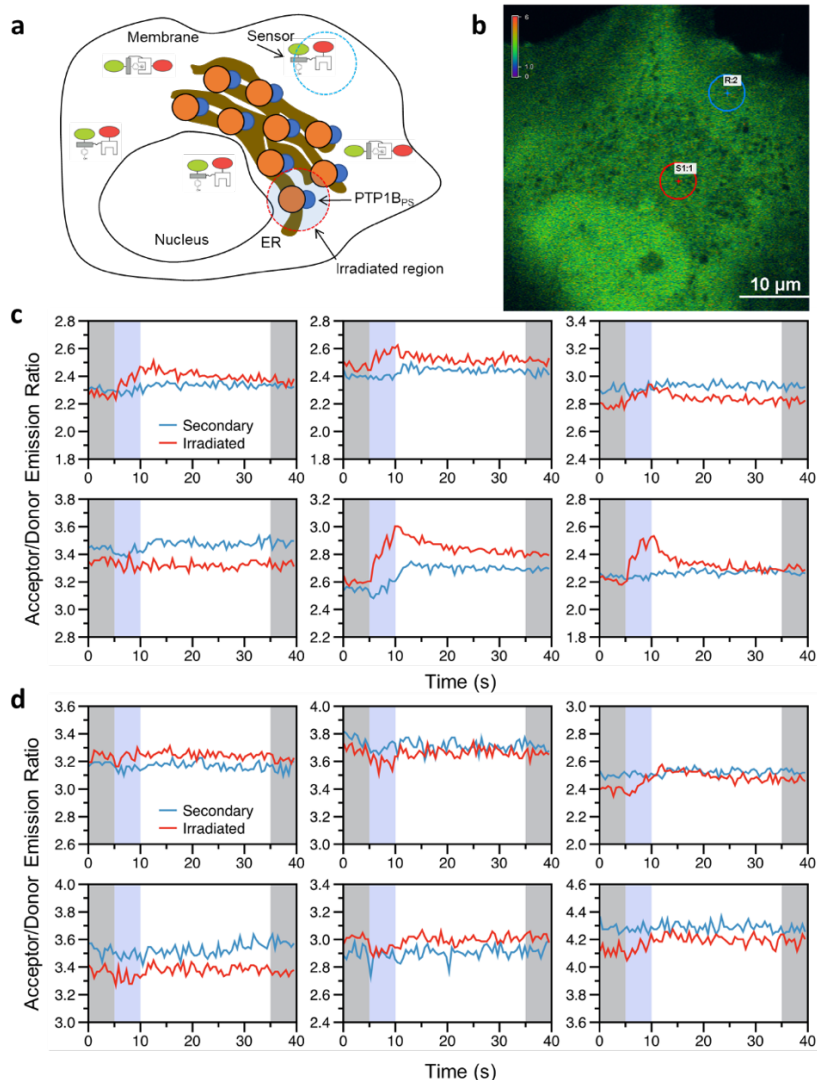


**Supplementary Figure 7 | Whole-cell irradiation of PTP1B<sub>PS</sub>\*\*.** **a**, A COS-7 cell expressing both PTP1B<sub>PS</sub>\*\* and a biosensor is irradiated with blue light (457 nm). Circles depict the irradiated region (light blue oval), a nuclear region (yellow circle, d = 5 μm), and a cytosolic region (green circle, d = 5 μm). **b**, The percent change in donor/acceptor emission ratio measured over 1 min within the nuclear and cytosolic regions. Each condition includes the interquartile average and SE for n = 11 biological replicates. Source data are provided as a Source Data file.

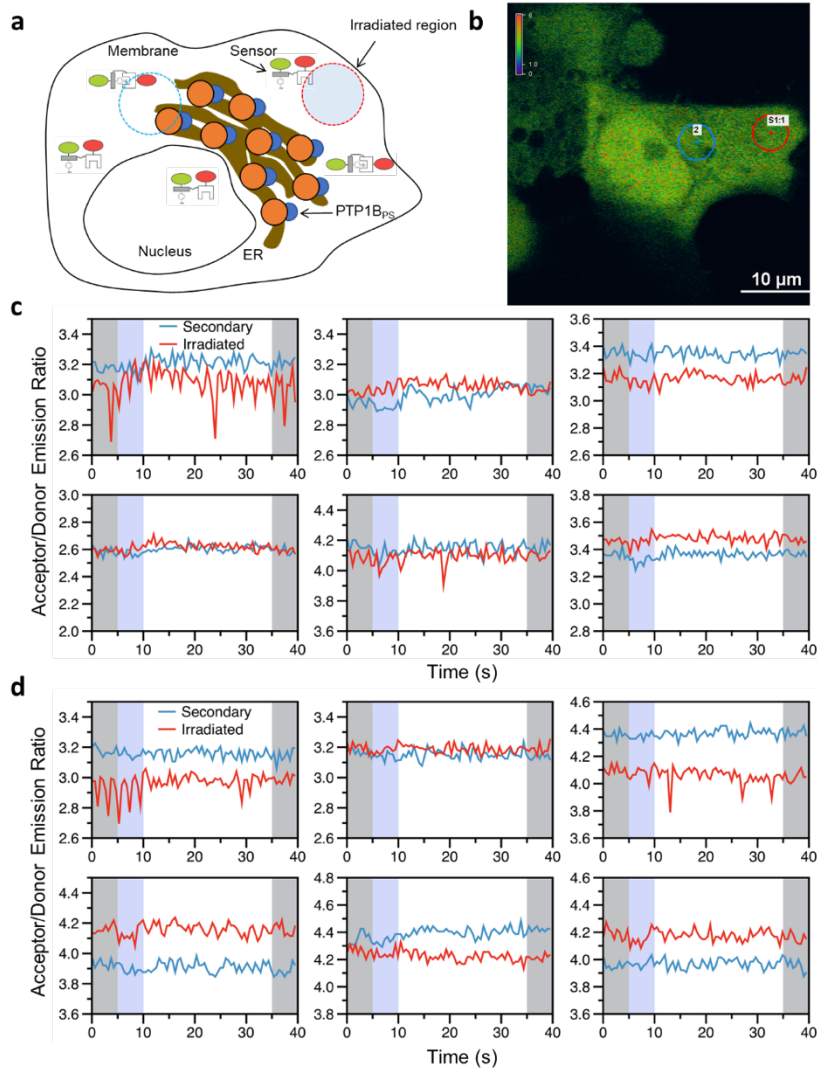


**Supplementary Figure 8 | Localized irradiation of PTP1BPs.** **a**, A COS-7 cell expressing both PTP1B<sub>PS</sub> and a biosensor is locally irradiated with 405-nm light. Circles depict the irradiated region (red with blue interior,  $d = 5 \mu\text{m}$ ) and a secondary region (blue,  $d = 5 \mu\text{m}$ ) in the cytosol. **b**, Image of a COS-7 cell expressing both PTP1B<sub>PS</sub> and a biosensor; circles show irradiated and secondary regions. **c**, Time courses of donor/acceptor emission ratios in each region. **d**, Time courses of emission ratios measured in locally irradiated COS-7 cells expressing both PTP1B<sub>PS</sub>(C450M) and the biosensor. In **c** and **d**, Shading highlights 5-s periods before (gray), during (blue), and after (gray) illumination. Source data are provided as a Source Data file.



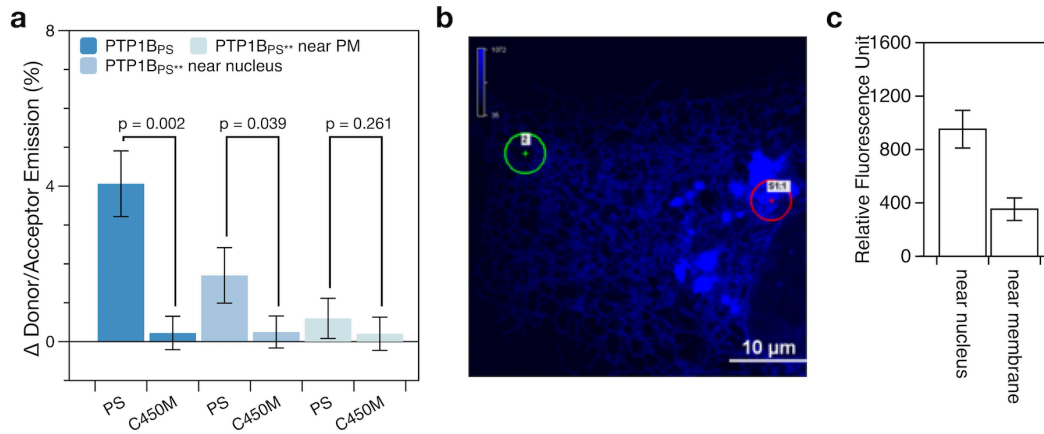


**Supplementary Figure 9 | Localized irradiation of PTP1B<sub>PS\*\*</sub> near the nucleus.** **a**, A COS-7 cell expressing both PTP1B<sub>PS\*\*</sub> and a biosensor is irradiated near the nucleus with 405-nm light. Circles depict the irradiated region (red with blue interior,  $d = 5 \mu\text{m}$ ) and a secondary region (blue,  $d = 5 \mu\text{m}$ ), both located within the cytosol. **b**, Image of a COS-7 cell expressing both PTP1B<sub>PS\*\*</sub> and a biosensor; circles depict the irradiated and secondary regions. **c**, Time courses of donor/acceptor emission ratios measured in both regions **b**. **d**, Time courses of donor/acceptor emission ratios measured in locally irradiated COS-7 cells expressing both PTP1B<sub>PS\*\*</sub>(C450M) and the biosensor. In **c** and **d**, Shading highlights 5-s periods before (gray), during (blue), and after (gray) illumination. Source data are provided as a Source Data file.

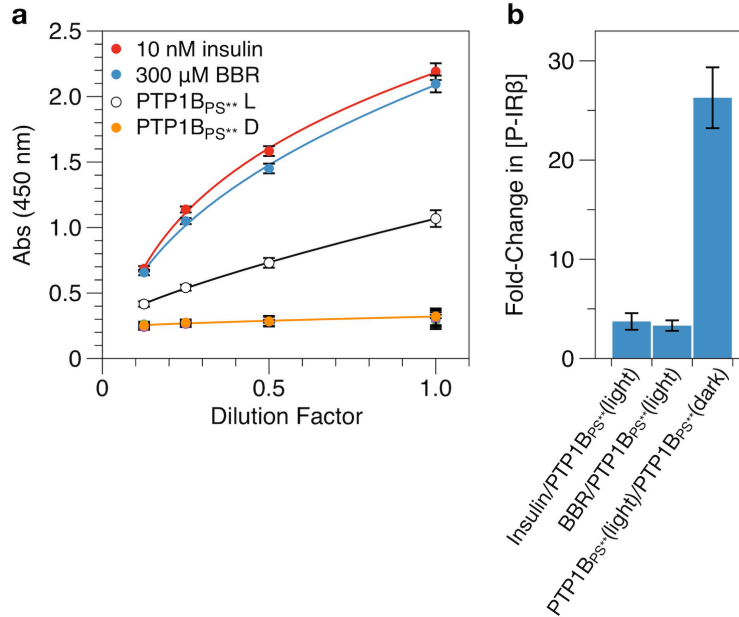


**Supplementary Figure 10 | Localized irradiation of PTP1B<sub>PS</sub>\*\* near the plasma membrane.**

**a**, A COS-7 cell expressing both PTP1B<sub>PS</sub>\*\* and a biosensor is irradiated near the plasma membrane with 405-nm light. Circles depict the irradiated region (red with blue interior,  $d = 5 \mu\text{m}$ ) and a secondary region (blue,  $d = 5 \mu\text{m}$ ) in the cytosol. **b**, Image of a COS-7 cell expressing both PTP1B<sub>PS</sub>\*\* and a biosensor. Circles ( $d = 5 \mu\text{m}$ ) show an irradiated region (red) and a secondary region (blue). **c**, Time courses of donor/acceptor emission ratios measured in both regions. **d**, Time courses of emission ratios measured in COS-7 cells expressing both PTP1B<sub>PS</sub>\*(C450M) and the biosensor. In **c** and **d**, Shading highlights 5-s periods before (gray), during (blue), and after (gray) illumination. Source data are provided as a Source Data file.



**Supplementary Figure 11 | Spatial heterogeneity of an ER-bound protein.** **a**, The change in FRET between 5-s intervals measured before and after illumination (gray regions in Figure 4e of the main text). For PTP1B<sub>PS</sub>\*, illumination near the nucleus, but not the plasma membrane (PM) causes a detectable change in FRET. **b**, Image of a COS-7 cell expressing an ER label<sup>6</sup>: BFP-Sec61β. Circular regions (d = 5 μm) appear near the nucleus (red) and plasma membrane (green). **c**, The average fluorescence of the nuclear region exceeds the average fluorescence of the membrane region by 2.7-fold, suggesting that the nuclear region contains more ER. Error bars denote SE for n = 6 (**a**) and n = 9 (**b**) biological replicates. Source data are provided as a Source Data file.



### Supplementary Figure 12 | Enzyme-linked immunosorbent assay (ELISA) of insulin

**receptor phosphorylation. a**, Measurements of insulin receptor phosphorylation (reported as a yellow color derived from 3,3',5,5'-tetramethylbenzidine) in cell lysate from either (i) HEK293T/17 cells exposed to 10 nM of insulin or 300 μM of BBR or (ii) PTP1B<sub>PS\*\*</sub>-expressing HEK293T/17 cells exposed to 455 nm light or kept in the dark. The dark dataset overlaps with those from (i) HEK293T/17 cells exposed to 1.5% DMSO (the concentration present in the BBR experiment) and (ii) PTP1B<sub>PS\*\*</sub>(C450M)-expressing HEK293T/17 cells exposed to 455 nm or kept in the dark. The overlap indicates that PTP1B<sub>PS\*\*</sub> does not alter the native phosphorylation state of its regulatory targets. Curves denote fits to the four-parameter logistic equation:  $y = d + (a - d) / (1 + (x/c)^b)$ , where  $y$  is absorbance at 450 nm, and  $x$  is the sample dilution (Supplementary Table 9). Error bars denote SE with  $n = 3$  biological replicates. **b**, Estimates of the difference in phosphorylated insulin receptor concentration between pairs of samples (Supplementary Table 10). Error bars represent SD of two independent estimates, each based on a separate standard curve from **a** (See Supplementary Note 2). Source data are provided as a Source Data file.

**Supplementary Table 1. Post-translational modifications of PTP1B.**

<i>Modification of PTP1B</i>	<i>Fold Change in Activity</i>	<i>Details of Measurement*</i>	<i>Reference</i>
<i>Insulin-stimulated phosphorylation of tyrosines and dephosphorylation of serines</i>	1.7-2.9 (inhibition)	Comparison of the activities of PTP1B immunoprecipitates collected from fat (2.9) and skeletal muscle (1.7) just before and 15 min after insulin stimulation of mice (Raytide-labeled substrate; p. 29523).	7
<i>Forskolin-stimulated phosphorylation of serines and dephosphorylation of tyrosines</i>	1.7-1.8 (activation)	Comparison of the activities of immunoprecipitates collected from fat (1.8) and skeletal muscle (1.7) in the presence and absence of forskolin, an activator of adenylyl cyclase (p. 29524).	7
<i>Calpain-mediated proteolysis of disordered C-terminus</i>	1.7 (activation)	Comparison of the activities of calpain-proteolyzed and wild-type PTP1B on p-nitrophenyl phosphate (p. 964).	8
<i>EGFR-mediated phosphorylation of Y66</i>	3.1 (activation)	Comparison of the activities of EGFR-phosphorylated PTP1B and PTP1B(Y66F) on pNPP (p. 144).	9
<i>PIAS1-mediated sumoylation of K335 and K347 (primary sites)</i>	2.3 (inhibition)	Comparison of the activities of PIAS1-sumoylated and wild-type PTP1B(1-403) on pNPP (p. 82).	10

\* Referenced figures and page numbers include descriptions of measurements and/or relevant source data; when necessary, we digitized the source data to obtain numerical values for DR by assuming a linear relationship between assay signal and enzyme activity.

**Supplementary Table 2. PTP1B-LOV2 Chimeras.**

Control	WT	Note	Ref
<b>Crossover</b>	1	Analysis of crossover location	N/A
	2	Analysis of crossover location	
	3	Analysis of crossover location	
	5	Analysis of crossover location	
	6	Analysis of crossover location	
	7	Analysis of crossover location	
	8	Analysis of crossover location	
	<b>Partition</b>	7.1	
7.2		Shortening of <u>S</u> HED <u>L</u> ATTLE ( $\alpha$ 7A' $\alpha$ ) to <u>S</u> HEATTLE	
7.3		Shortening of <u>S</u> HED <u>L</u> ATTLE ( $\alpha$ 7A' $\alpha$ ) to <u>S</u> HATTLE	
7.4		Shortening of <u>S</u> HED <u>L</u> ATTLE ( $\alpha$ 7A' $\alpha$ ) to <u>S</u> ATTLE	
7.5		Shortening of <u>S</u> HED <u>L</u> ATTLE ( $\alpha$ 7A' $\alpha$ ) to ATTLE	
7.6		Shortening of <u>S</u> HED <u>L</u> ATTLE ( $\alpha$ 7A' $\alpha$ ) to <u>S</u> HED <u>L</u> TLE	
7.7		Shortening of <u>S</u> HED <u>L</u> ATTLE ( $\alpha$ 7A' $\alpha$ ) to <u>S</u> HED <u>L</u> TLE	
7.8		Shortening of <u>S</u> HED <u>L</u> ATTLE ( $\alpha$ 7A' $\alpha$ ) to <u>S</u> HED <u>L</u> LE	
7.9		Shortening of <u>S</u> HED <u>L</u> ATTLE ( $\alpha$ 7A' $\alpha$ ) to <u>S</u> HED <u>L</u> E	
7.10		Shortening of <u>S</u> HED <u>L</u> ATTLE ( $\alpha$ 7A' $\alpha$ ) to <u>S</u> HED <u>L</u>	
<b>J<math>\alpha</math></b>	7.1(L514A)	Stabilization of J $\alpha$ helix	
	7.1(G528A)	Stabilization of J $\alpha$ helix	
	7.1(G528A/N538E)	Stabilization of J $\alpha$ helix	
	7.1 $\Delta$ J $\alpha$	Removal of J $\alpha$ helix	
	7.1(I532E)	Destabilization of J $\alpha$ helix	
	7.1(I539E)	Destabilization of J $\alpha$ helix	
<b>A'<math>\alpha</math></b>	7.1(T406A)	Stabilization of A' $\alpha$ helix	
	7.1(T407A)	Stabilization of A' $\alpha$ helix	
	7.1(T406A/T407A)	Stabilization of A' $\alpha$ helix	
	7.1(L408D)	Destabilization of A' $\alpha$ helix	
<b><math>\alpha</math>7</b>	7.1(H296A)	Stabilization of A' $\alpha$ helix	
	7.1(E297A)	Stabilization of A' $\alpha$ helix	
	7.1(D298A)	Stabilization of A' $\alpha$ helix	
	7.1(S296A)	Stabilization of A' $\alpha$ helix	
	7.1(D289A)	Stabilization of A' $\alpha$ helix	
	7.1(K292A)	Stabilization of A' $\alpha$ helix	
	7.1(E293A)	Stabilization of A' $\alpha$ helix	
<b>Combination</b>	7.1(S286A/T406A)	Stabilization of $\alpha$ 7A' $\alpha$ overlap	
	7.1(K292A/T406A)	Stabilization of $\alpha$ 7A' $\alpha$ overlap	
	7.1(S296A/K292A)	Stabilization of $\alpha$ 7A' $\alpha$ overlap	
	7.1(S286A/K292A/T406A)	Stabilization of $\alpha$ 7A' $\alpha$ overlap	
	7.1(H296A/T406A)	Stabilization of $\alpha$ 7A' $\alpha$ overlap	
<b>Allostery</b>	7.1(Y152A/Y153A)	Destabilization of allosteric control	
<b>Photoinactive mutant</b>	7.1(C450M)	Inactivation of photoswitching	

**Supplementary Table 3. Primers used to assemble PTP1B-LOV2 chimeras.**

#	<i>PTP1B</i>		<i>LOV2</i>	
	F Primer	R Primer	F Primer	R Primer
1	aaaaaccatggagatgga aaaggagttcgagc	ccgccttagctcatcatcaaac tctcgtcccccattgatgaattgg cac	gtgccaaatcatcatgggggac gagagtttggatgatgagctaagg cgg	ttttggatcctcagtggtggtgg tgggtggtcctcgagaagttcttt gccgcctcatcaat
2	aaaaaccatggagatgga aaaggagttcgagc	catttcttccgccttagctcatca tcaaaggaagagtcctccatga tgaattgg	ccaaatcatcatgggggactctt cctttgatgatgagctaagcgga aagaaatg	ttttggatcctcagtggtggtgg tgggtggtcctcgagaagttcttt gccgcctcatcaat
3	aaaaaccatggagatgga aaaggagttcgagc	cttctcatttcttccgccttagctc atcctgcacggaagagtccc	gggactcttccgtgcaggatgag ctaaggcggaaagaaatgagaa g	ttttggatcctcagtggtggtgg tgggtggtcctcgagaagttcttt gccgcctcatcaat
5	aaaaaccatggagatgga aaaggagttcgagc	gtagtagccaagtctataccctt ctcatctcctccactgatcctgc acg	cgtagcaggatcagtggaaggag atgagaagggtatagactggct actac	ttttggatcctcagtggtggtgg tgggtggtcctcgagaagttcttt gccgcctcatcaat
6	aaaaaccatggagatgga aaaggagttcgagc	gtgtagtagccaagtctataccc cttctaagctcctccactgatcct gc	gcaggatcagtggaaggagctta gaaggggtatagacttggtacta cac	ttttggatcctcagtggtggtgg tgggtggtcctcgagaagttcttt gccgcctcatcaat
7	aaaaaccatggagatgga aaaggagttcgagc	gttcttcaatacgttcaagtgtg gtagccaggtcctcgtgggaaa gctc	gagcttcccacaggacctggc factacacttgaacgtattgagaa aac	ttttggatcctcagtggtggtgg tgggtggtcctcgagaagttcttt gccgcctcatcaat
8	aaaaaccatggagatgga aaaggagttcgagc	gggtcagtaatgacaagtctt ctcaatacgtcctgggtgggggc tccag	ctggagccccaccgagcgtat tgagaagaacttgtcattactgac cc	ttttggatcctcagtggtggtgg tgggtggtcctcgagaagttcttt gccgcctcatcaat
7.1	aaaaaccatggagatgga aaaggagttcgagc	gttcttcaatacgttcaagtgtg gtagcgtcctcgtgggaaagct cc	gga gct ttc cca cga gga c gctactacacttgaacgtattgag aagaac	ttttggatcctcagtggtggtgg tgggtggtcctcgagaagttcttt gccgcctcatcaat
7.2	aaaaaccatggagatgga aaaggagttcgagc	gttcttcaatacgttcaagtgtg gtagcctcgtgggaaagctcctt cc	ggaaggagcttcccacgag gctactacacttgaacgtattgag aagaac	ttttggatcctcagtggtggtgg tgggtggtcctcgagaagttcttt gccgcctcatcaat
7.3	aaaaaccatggagatgga aaaggagttcgagc	gttcttcaatacgttcaagtgtg gtagcgtgggaaagctccttcc actg	cagtggaaggagcttcccac gctactacacttgaacgtattgag aagaac	ttttggatcctcagtggtggtgg tgggtggtcctcgagaagttcttt gccgcctcatcaat
7.4	aaaaaccatggagatgga aaaggagttcgagc	gttcttcaatacgttcaagtgtg gtagcggaaagctccttccactg atcc	ggatcagtggaaggagcttcc gctactacacttgaacgtattgag aagaac	ttttggatcctcagtggtggtgg tgggtggtcctcgagaagttcttt gccgcctcatcaat
7.5	aaaaaccatggagatgga aaaggagttcgagc	gttcttcaatacgttcaagtgtg gtagcaagctcctccactgatc ctgc	gcaggatcagtggaaggagctt gctactacacttgaacgtattgag aagaac	ttttggatcctcagtggtggtgg tgggtggtcctcgagaagttcttt gccgcctcatcaat
7.6	aaaaaccatggagatgga aaaggagttcgagc	caaagtcttcaatacgttcaa gtgtagtcaggtcctcgtgggaa agc	gcttcccacgaggacctg actacacttgaacgtattgagaag aactttg	ttttggatcctcagtggtggtgg tgggtggtcctcgagaagttcttt gccgcctcatcaat

**Supplementary Table 3 (continued). Primers to assemble PTP1B-LOV2 chimeras.**

#	<i>PTP1B</i>		<i>LOV2</i>	
	F Primer	R Primer	F Primer	R Primer
7.7	aaaaccatggagatgga aaaggagtcgagc	gacaaagttctcaatacgttc aaggtgcaggctcctcgtggaa agc	gctttccacgaggacctg acactgaacgtattgagaagaac tttgc	ttttggatcctcagtggtggtggt ggtggtgctcgagaagttctttgc cgctcatcaat
7.8	aaaaccatggagatgga aaaggagtcgagc	cagtaatgacaaagttctctcaa tacgttcaagcaggctcctcgtgg gaaagc	gctttccacgaggacctg cttgaacgtattgagaagaactttg tcattactg	ttttggatcctcagtggtggtggt ggtggtgctcgagaagttctttgc cgctcatcaat
7.9	aaaaccatggagatgga aaaggagtcgagc	gtcagtaatgacaaagttctctc aatacgttccaggctcctcgtggg aaagc	gctttccacgaggacctg gaacgtattgagaagaactttgtc attactgac	ttttggatcctcagtggtggtggt ggtggtgctcgagaagttctttgc cgctcatcaat
7.10	aaaaccatggagatgga aaaggagtcgagc	ggcagtaatgacaaagttctctc caatacgcaggctcctcgtggga aagc	gctttccacgaggacctg cgtattgagaagaactttgctatta ctgacc	ttttggatcctcagtggtggtggt ggtggtgctcgagaagttctttgc cgctcatcaat
7.1A $\alpha$	aaaaccatggagatgga aaaggagtcgagc	gttcttcaatacgttcaagtgtgta gtagcgtcctcgtgggaaagct cc	gga gct ttc cca cga gga c gctactacactgaacgtattgag aagaac	ttttggatcctcagtggtggtggt ggtggtgctcgaggacatgctca gttccatccaa
<i>PTP1B</i> <sub>281</sub>	aaaaccatggagatgga aaaggagtcgagc	ttttggatcctcaatgatgatgat gatgatgctcgaggatgaatttg gcaccttcgatcac	N/A	N/A



**Supplementary Table 4. Primers used for site-directed mutagenesis.**

<i>Mutant</i>	<i>F Primer</i>	<i>R Primer</i>
7.1(L514A)	gtccagtactttattggggtcaggcggatggaactgagcatgtccgagat	atctcggacatgctcagttccatccgcctgaacccaataaagtactggac
7.1(G528A)	gtccgagatgctgccgagagagaggcagtcagctgattaagaaaactgca	tgcagtttcttaacagcatgactgcctctctcggcagcatctcggac
7.1(G528A/N538E)	gtccgagatgctgccgagagagaggcagtcagctgattaagaaaactgca/atgctgattaagaaaactgcagaagagattgatgaggcggcaaaagaactt	tgcagtttcttaacagcatgactgcctctctcggcagcatctcggac/aagttctttgccgcctcatcaatctctctgcagtttcttaacagcat
7.1(I532E)	gccgagagagaggagtcagctgctggagaagaaaactgcagaaaattgat	atcaatattttctgcagtttctctccagcatgactccctctctcggc
7.1(I539E)	ctgattaagaaaactgcagaaaatgaggatgaggcggcaaaagaactctc	gagaagtcttttggcgcctcatcctcatttctgcagtttcttaacag
7.1(T406A)	agctttcccacgaggacgctgctacactgaacgtattgagaa	ttctcaatacgttcaagtgtagcagcgtcctcgtgggaaagct
7.1(T407A)	ttcccacgaggacgctactgcaactgaacgtattgagaagaa	ttcttcaatacgttcaagtgcagtagcgtcctcgtgggaaa
7.1(T406A/T407A)	gagctttcccacgaggacgctgctgcaactgaacgtattgagaagaactt	aaagtctctcaatacgttcaagtgcagcagcgtcctcgtgggaaagctc
7.1(L408D)	cttcccacgaggacgctactacagatgaacgtattgagaagaactttgct	gacaaagtcttctcaatacgttcatctgtagtagcgtcctcgtggaaag
7.1(H296A)	atcagtggaaggagcttccgcagaggacgctactacacttga	tcaagtgtagtagcgtcctcgtgggaaagctccttccactgat
7.1(E297A)	agtggaaggagcttcccacgcagacgctactacacttgaacg	cgttcaagtgtagtagcgtcgtgggaaagctccttccactg
7.1(D298A)	ggaaggagcttcccacgaggcagctactacacttgaacgtat	atacgttcaagtgtagtagcgtcgtgggaaagctccttcc
7.1(S286A)	gccaaattcatcatggggactctgccgtgcaggatcagtggaaggagctt	aagctccttccactgatcctgcacggcagagtccccatgatgaattggc
7.1(D289A)	atcatggggactctccgtgcaggctcagtggaaggagcttcccacgag	ctcgtgggaaagctccttccactgagcctgcacggagagtcccccatgat
7.1(K292A)	gactctccgtgcaggatcagtgggcggagcttcccacgagacgctact	agtagcgtcctcgtgggaaagctccgccactgatcctgcacggaagagtc
7.1(E293A)	tcttcgtgcaggatcagtggaaggcgttcccacgaggacgctactaca	tgtagtagcgtcctcgtgggaaagcgttccactgatcctgcacggaaga
7.1(S286A/T406A)	gccaaattcatcatggggactctgccgtgcaggatcagtggaaggagctt/agcttcccacgaggacgctgctacacttgaacgtattgagaa	aagctccttccactgatcctgcacggcagagtccccatgatgaattggc/ttctcaatacgttcaagtgtagcagcgtcctcgtgggaaagct
7.1(K292A/T406A)	gactctccgtgcaggatcagtgggcggagcttcccacgagacgctact/gcggagcttcccacgaggacgctgctacacttgaacgtattgagaaga	agtagcgtcctcgtgggaaagctccgccactgatcctgcacggaagagtc/gtcttcaatacgttcaagtgtagcagcgtcctcgtgggaaagctcctcgc

**Supplementary Table 4 (continued). Primers used for site-directed mutagenesis.**

<i>Mutant</i>	<i>F Primer</i>	<i>R Primer</i>
7.1(S286A/K292A)	gccaaattcatcatgggggactctgccgtgcaggatcagtggaaggagctt/ gactctgccgtgcaggatcagtgggcggagctttccacgaggacgctact	aagctccttccactgatcctgcacggcagagtccccatgatgaatttggc/ agtagcgtcctcgtgggaaagctccgccactgatcctgcacggcagagtc
7.1(S286A/K292A/T406A)	gccaaattcatcatgggggactctgccgtgcaggatcagtggaaggagctt/gactctgccgtgcaggatcagtgggcggagctttccacgaggacgctact/ gctgagctttccacgaggacgctgctacactgaacgtattgagaagaac	aagctccttccactgatcctgcacggcagagtccccatgatgaatttggc/ agtagcgtcctcgtgggaaagctccgccactgatcctgcacggcagagtc/ gttcttcaatacgttcaagttagcagcgtcctcgtgggaaagctccgc
7.1(H296A/T406A)	caggatcagtgaaggagctttccgccgaggacgctgctacacttgaacgt /agctttccacgaggacgctgctacactgaacgtattgagaa	acgttcaagttagcagcgtcctcggcggaaagctcctccactgacctg /tttcaatacgttcaagttagcagcgtcctcgtgggaaagct
7.1(Y152A/Y153A)	ttgatctctgaagatatcaagtcagcttatacagtcgcacagctgaattg	caattctagctgtcgcactgtataagctgacttgatatcttcagatca
7.1(C450M)	cgtgaagaaatttgggaagaaacatgaggtttctacaagctctgaaact	agtttcaggacctgtagaacacctatgtttctccaaaatttctcacg
<i>PTP1B<sub>PS</sub>*</i> (L514A)	gtccagtactttattggggtcaggcggatggaactgagcatgctcgagat	atctcggacatgctcagttccatccgcctgaacccaataaagtactggac
<i>PTP1B<sub>PS</sub>*</i> (G528A/N538E)	gtccgagatgctccgagagagaggcagtcagctgattaagaaaactgca/atgctgattaagaaaactgcagaagagattgatgagcggc gcaaaagaactt	tgcagtttcttaacagcatgactgcctctctcggcagcatctcggac/aagtcttttggcgcctcatcaatctctcagatttcttaacagcat

**Supplementary Table 5. Primers used for variants of GFP-tagged PTP1B<sub>PS</sub>.**

<i>Mutant</i>	<i>F Primer</i>	<i>R Primer</i>
<i>PTP1B<sub>PS</sub></i>	aaaaagaattcaatggagatggaaaaggagttcgagc	gaaaatattgatgagcgcgaaaagaacttgatccaaaa
<i>PTP1B<sub>PS**</sub></i>	aaaaagaattcaatggagatggaaaaggagttcgagc	ttttggatccctatgtgtgctgttgaacggaacctgtagcag aggtaagcgcc
<i>PTP1B<sub>435</sub></i>	aaaaagaattcaatggagatggaaaaggagttcgagc	ttttggatccctatgtgtgctgttgaacggaacctgtagcag aggtaagcgcc

**Supplementary Table 6. Primers used for Gibson assembly.**

#	<i>F Primer</i>	<i>R Primer</i>
<i>Pc#1-Biosensor</i>	ggctgctaacaagcccgaaag	acatgatgatgatgatgatgcatggtatatac
<i>Pc#2-Biosensor</i>	catcatcatcatcatcatgtgagcaagg gcgaggag	tgatcttcccaaaataccactgtacagctcgtccatg cc
<i>Pc#3-Biosensor</i>	tggatatttgggaagatcactcgtc	gagctcccctgtaggtgg
<i>Pc#4-Biosensor</i>	tacagggggagctcgtgtctaagggcg aagagctg	gctttgttagcagccttactgtacagctcgtccatccc
<i>Pc#1-PTP1B<sub>PS*</sub></i>	gcggcaaaagaacttctggagccccca cccg	atgatgatgatgctcgaggtaactcagtgcattgctc tcgtc
<i>Pc#2-PTP1B<sub>PS*</sub></i>	ctcgagcatcatcatcatcattgagg	aagttctttgccgcctcatcaat
<i>Pc#3-PTP1B<sub>PS*</sub></i>	tccagtgatcgaagttaggctgg	ctaactcgatcactggaccgctg
<i>Pc#1-Biosensor-P2A-PTP1B<sub>PS</sub></i>	ggtggcgaccggtagcg	ctgatcataatcagccataccacattgtagag
<i>Pc#2-Biosensor-P2A-PTP1B<sub>PS</sub></i>	ggcagcggcgccacc	gcttttctgctcccacacatctc
<i>Pc#3- Biosensor-P2A-PTP1B<sub>PS</sub></i>	tgggagcagaaaagcaggggtgctgt catgctcaac	gtatggctgattatgatcagttaaagtctttgccgcc tcatcaatatttc
<i>Pc#4- Biosensor-P2A-PTP1B<sub>PS</sub></i>	ccggtgccaccatggtgagcaaggg cgaggagc	cgccgctgccctgtacagctcgtccatcccac
<i>Pc#4- Biosensor-P2A-PTP1B<sub>PS**</sub></i>	ccggtgccaccatggtgagcaaggg cgaggagc	atggctgattatgatcagttatgtgtgctgttgaacag gaacc

Note: Pc#1 denotes the first piece of a Gibson assembly.

## Supplementary Table 7. DNA fragments used for Gibson assembly

#	<i>DNA sequence</i>
<i>P2A-PTP1B</i>	ggcagcggcgccaccaacttctccctgctgaagcaggccggcgacgtggaggagaacccggc cccatggagatggaaaaggagttcgagcagatcgacaagtccgggagctggcgccattfacca ggatatccgacatgaagccagtgacttccatgtagagtggccaagcttctaagaacaaaaaccga aataggtacagagacgtcagtcctttgaccatagtcggattaactacatcaagaagataatgactat atcaacgctagttgataaaaatggaagaagccaaaggagttacattctaccagggccttgcct aacacatcggtcacttttgggagatggtgtgggagcagaaaagc

**Supplementary Table 8. Optogenetic Constructs**

Protein*	Light-sensitive Moiety	Mechanism	Dynamic Range (DR)	Assay for DR**	Cellular Response**	Ref
Pyruvate kinase M2 isoform	LOV2 from <i>A. sativa</i> phototropin I	Optically induced conformational change in LOV2 causes an activity-distorting conformational change in an enzyme.	1.4-1.9 (activation)	Pyruvate production (in the presence and absence of light) measured by time-resolved series of <sup>1</sup> H-NMR spectra (p. 2966).	In the presence of [U C-13] glucose, irradiation of HeLa cells increased C-13 incorporation into pyruvate (52% in light vs. 35% in dark; p. 2966).	11
RhoA GTPase	LOV2 from <i>A. sativa</i> phototropin I	Optically induced conformational change in LOV2 causes an activity-distorting conformational change in an enzyme.	1.7 (inhibition)	Biosensor-based quantification (i.e., FRET) of GTPase activity in HeLa cells for dark- and light-state mutants of LOV2 (p. 1442).	Irradiation of fibroblasts showed increased protrusions upon irradiation (Supplementary Fig. 13).	12
Peptide inhibitor of protein kinase A (PKA)	LOV2 from <i>A. sativa</i> phototropin I	Optically induced unwinding of the J $\alpha$ exposes an attached inhibitory peptide.	1.9 (inhibition / binding)	Quantification of a Western blot showing the phosphorylation state of a PKA substrate before/after illumination (p. 790).	Irradiation of cells caused 2-fold reduction in forskolin-dependent phosphorylation of ERB (p. 790).	13
Vav2 GTP exchange factor	LOV2 from <i>A. sativa</i> phototropin I	Optically induced conformational change in LOV2 causes an activity-distorting conformational change in an enzyme.	2.1 (inhibition)	Biosensor-based quantification (i.e., FRET) of Rac1 GTPase activity in HeLa cells for dark- and light-state mutants of LOV2 (p. 1443).	Irradiation of HeLa cells produced rapid reversible retraction (p. 1443).	12
Nuclear export sequence	LOV2 from <i>A. sativa</i> phototropin I	Optically induced unwinding of an internal J $\alpha$ -A' $\alpha$ connection within a LOV2-LOV2 fusion exposes an embedded nuclear export sequence that can bind to CRM1.	2.3 (binding)	Quantification of optically induced relocalization of a fluorescent protein from the nucleus to the cytosol (p. 399).	N/A	14
Peptide binding partner of engineered PDZ domain.	LOV2 from <i>A. sativa</i> phototropin I	Optically induced unwinding of the J $\alpha$ helix uncages a peptide epitope and enables binding to a cognate PDZ domain.	2.7 (binding)	Quantification of optically induced relocalization from the cytosol to the plasma membrane (Supplementary Fig. 6).	Irradiation of HeLa cells enabled localization of ePDZb1-mCherry to the plasma membrane and outer membrane of the mitochondria (p. 380).	15

Protein*	Light-sensitive Moiety	Mechanism	Dynamic Range (DR)	Assay for DR**	Cellular Response**	Ref
Src kinase	LOV2 from <i>A. sativa</i> phototropin I	Optically induced conformational change in LOV2 causes an activity-distorting conformational change in an enzyme.	3.0-5.2 (inhibition)	Quantification of (i) paxillin phosphorylation in <i>in vitro</i> assay (5.2) and (ii) tyrosine phosphorylation in cell lysate (3.0) before/after illumination (p. 1442).	Irradiation of SYF cells caused Src to translocate to focal adhesions; edge movements tended to increase, and cells polarized (p. 1442).	12
Peptide inhibitor of myosin light chain kinase	LOV2 from <i>A. sativa</i> phototropin I	Optically induced unwinding of the $\alpha$ exposes an attached inhibitory peptide.	3.3 (inhibition / binding)	Quantification of a Western blot showing the phosphorylation state of myosin light chain before/after illumination (p. 791).	Irradiation of cells caused a statistically significant reduction in membrane protrusion velocity (p. 791).	13
Cdc42 GTPase	LOV2 from <i>A. sativa</i> phototropin I	Optically induced conformational change in LOV2 causes an activity-distorting conformational change in an enzyme.	3.5 (inhibition)	Biosensor-based quantification (i.e., FRET) of GTPase activity in HeLa cells for dark- and light-state mutants of LOV2 (p. 1442).	Irradiation of fibroblasts produced retraction and an accumulation of actin at the cell periphery (Supplementary Fig. 13).	12
BphP1 from <i>Rhodospseudomonas palustris</i>	BphP1 from <i>Rhodospseudomonas palustris</i>	Optically induced conformational change in BphP1 changes its affinity for its binding partner PpsR2	3.5 (binding)	Binding: Quantification of optically induced relocalization of a fluorescent protein from the cytosol to the nucleus (p. 594).	Irradiation of HeLa cells enabled 40-fold higher expression of SEAP under 740 nm light than in the dark (p. 594). Note: Transcription and translation are amplification reactions.	16
Nuclear export sequence	LOV2 from <i>A. sativa</i> phototropin I	Optically induced unwinding of the $\alpha$ exposes an embedded nuclear export sequence that can bind to CRM1.	4 - 14 (binding)	Quantification of optically induced relocalization of a fluorescent protein from the nucleus to the cytosol (p. 399). The dynamic range differed between NESSs.	Illumination of yeast cells expressing Bre1 bound to the photoswitchable construct caused a measurable decrease in H2B histone ubiquitylation (p. 400).	14
Rac1 GTPase	LOV2 from <i>A. sativa</i> phototropin I	Optically induced conformational change in LOV2 causes an activity-distorting conformational change in an enzyme.	4.5 (inhibition)	Biosensor-based quantification (i.e., FRET) of GTPase activity in HeLa cells for dark- and light-state mutants of LOV2 (p. 1442).	Irradiation of fibroblasts caused reversible cell edge retraction and broad retraction of entire lamellae (p. 1443).	12

Protein*	Light-sensitive Moiety	Mechanism	Dynamic Range (DR)	Assay for DR**	Cellular Response**	Ref
Fibroblast growth factor receptor 1 (FGFR1)	LOV from <i>V. frigida</i> aureochrome I	Optically induced dimerization of LOV2 induces dimerization--and activation--of the RTKs to which they are attached.	5.5 (activation / transcription)	Quantification of MAPK/ERK pathway activation and subsequent luciferase expression (reporter) in HEK293 cells in response to blue light (p. 1716).	Irradiation of M38K cells induced phosphorylation of the receptor and ERK1/2 and caused an increase in cell proliferation and induced EMT-like morphological and gene expression changes (p. 1718).	17
<i>trp</i> repressor from <i>E. coli</i>	LOV2 from <i>A. sativa</i> phototropin I	Optically induced unwinding of the $\alpha$ helix causes TrpR domains to adopt conformations that enable binding to DNA.	5.6 (binding)	Binding affinity measured through the quantification of RsaI protection by Trp in the presence and absence of light (p. 10712).	N/A	18
Adenylate cyclase (AC) from <i>Nostoc</i> sp.	BphG1 from <i>Rhodobacter sphaeroides</i>	Optically induced dimerization of BphG1 induces dimerization of AC, which functions as a homodimer.	5.7 (activation / binding)	<i>In vitro</i> measurement of the kinetics of cAMP accumulation in the presence and absence of light (p. 10170)	Cholinergic neurons expressing the photoswitchable AC exhibited a higher frequency of body bends in the presence of red light (relative to the dark, p. 10170).	19
Cas9 endonuclease	LOV2 domain from <i>Rhodobacter sphaeroides</i>	Optically induced dissociation of a LOV2 dimer uncages a variant of Cas9 with LOV2 embedded within it, enabling endonuclease activity.	6.5 (activation, transcription)	Quantification of dCas9-mediated transcriptional repression of RFP gene (p. 10006).	Irradiation of <i>E. coli</i> harboring photoswitchable cas9 yielded 3-fold repression of endogenous <i>lacZ</i> (p. 10011).	20
Raf1 kinase	Dronpa from <i>Pectinidae</i> coral	Optically induced dissociation of a Dronpa dimer uncages the active site.	6.8 (activation)	Quantification of a Western blot showing the light-dependent phosphorylation ERK (p. 2).	A pulse of 500-nm light elicited transient increase in MEK phosphorylation, evidencing negative feedback on Raf activity (p. 4). Exposure of <i>C. elegans</i> to 500-nm light led to tail swelling with 73-79% penetrance (p. 5).	21

Protein*	Light-sensitive Moiety	Mechanism	Dynamic Range (DR)	Assay for DR**	Cellular Response**	Ref
AcrIIA4 from <i>I. monocytophages</i>	LOV2 from <i>A. sativa</i> phototropin I	Optically induced conformational change in LOV2 causes an activity-distorting conformational change in AcrIIA4, reducing its ability to inhibit Cas9.	7.4 (unbinding, transcription)	Quantification of dCas9-mediated transcriptional repression of luciferase gene in HEK293T cells (p. 925).	Irradiation of HEK293T cells yielded light-dependent insertion/deletion (indel) mutations (p. 925) and light-dependent telomere recruitment (p. 927)	22
SsrA peptide	LOV2 from <i>A. sativa</i> phototropin I	Optically induced unwinding of the $\alpha$ exposes an embedded inhibitory peptide.	8 (binding)	Dark- and light-state binding affinity measured with a fluorescence polarization competition assay (p. 511).	N/A	23
MEK2 kinase	Dronpa from <i>Pectinidae</i> coral	Optically induced disassociation of a Dronpa dimer uncages the active site.	8.6 (activation)	Quantification of a Western blot showing the light-dependent phosphorylation ERK (p. 2).	N/A	21
MEK1 kinase	Dronpa from <i>Pectinidae</i> coral	Optically induced dissociation of a Dronpa dimer uncages the active site.	9.1 (activation)	Quantification of a Western blot showing the light-dependent phosphorylation ERK (p. 2).	Irradiation of cells with 500-nm light induced translocation of ERK KTR-mRuby2 from nucleus to cytosol; irradiation with 400 nm light reversed this effect (p. 2). Exposure of <i>C. elegans</i> to 500-nm light produced tail swelling with 73-79% penetrance (p. 5).	21
Rac1 GTPase	LOV2 from <i>A. sativa</i> phototropin I	Optically induced unwinding of the $\alpha$ exposes active site of GTPase.	10 (activation)	Binding affinity for PAK measured with isothermal titration calorimetry on light- and dark-state mutants (p. 104).	Irradiation of HeLa cells produced lamellipodial protrusions and membrane ruffles (p. 104). Irradiation of MEF cells at a spot near the cell edge produces local protrusion and distal retraction (p. 104).	1
Cre Recombinase	Cryptochrome 2 from <i>A. thaliana</i>	Optically induced dimerization of Cry2 and CIB permits assembly of a split recombinase.	13.7 (activation)	Quantification of Cre recombinase activity in HEK293 cells pulsed with light (p. 428).	Brief irradiation of HEK293 cells enabled a ~14% increase in recombination (relative to the dark; p. 428).	24



Protein*	Light-sensitive Moiety	Mechanism	Dynamic Range (DR)	Assay for DR**	Cellular Response**	Ref
Peptide binding partner (SsrA) of SspB.	LOV2 from <i>A. sativa</i> phototropin I	Optically induced unwinding of the $\alpha$ helix uncages the SsrA peptide, allowing it to bind to SspB.	36 (binding)	Light- and dark-state binding affinity for SspB measured with a fluorescence polarization competition assay (p. 114).	Irradiation of fibroblasts expressing mitochondria-anchored LOV2-SsrA caused recruitment of SspB (page 115). Irradiation of fibroblasts expressing (i) membrane-anchored LOV2-SsrA and (ii) a fusion of the DH/PH domain of Tiam1 to the N-terminus of TagRFP-SspB produced ruffles and lamellipodia formation (p. 116).	25
Vinculin-binding peptide from ipaA	LOV2 from <i>A. sativa</i> phototropin I	Optically induced unwinding of the $\alpha$ exposes an embedded inhibitory peptide.	49 (binding)	Dark- and light-state binding affinity measured with a fluorescence polarization competition assay (p. 511).	Irradiation of <i>S. cerevisiae</i> expressing (i) LOV-ipaA linked to the Gal4 activation domain and (ii) vinculin D1 to the Gal4 binding domain enabled 12-fold higher expression of LacZ (relative to dark; p. 513).	23
LOV2 from <i>A. sativa</i> phototropin I	LOV2 from <i>A. sativa</i> phototropin I	Optically induced unwinding of the $\alpha$ helix prevents binding to Zdk, a protein evolved to bind the dark-state of LOV2.	> 150 (binding)	Binding affinity of dark- and light-state mutants measured with radiometric binding assay (p. 755).	Irradiation of HeLa cells expressing both (i) Zdk bound to constitutively active mutants of RhoA, Rac1, and Vav2 and (ii) mitochondria-localized LOV2 caused changes in edge velocity, ruffling, cell area, and protrusion distribution (p. 757).	26

†This table provides a reference set of optogenetic constructs, each chosen for its reliance on a LOV domain or for its demonstrated use in signaling studies.

\*Constructs in which the light-sensitive moiety exerts direct control over enzyme activity appear in blue; constructs in which the moiety controls protein-protein interactions appear in orange.

\*\* Referenced figures and page numbers include descriptions of measurements and/or relevant source data; when necessary, we digitized the source data to obtain numerical values for DR.

**Supplementary Table 9. Four-parameter logistic regression**

<i>Parameter*</i>	<i>PTP1B<sub>PS**</sub></i> <i>(light)</i>	<i>Insulin</i> <i>(10 nM)</i>	<i>BBR</i> <i>(300 μM)</i>	<i>PTP1B<sub>PS**</sub></i> <i>(dark)</i>
<b><i>a</i></b>	0.247	-1.427	-0.370	0.234
<b><i>b</i></b>	0.753	0.279	0.419	0.675
<b><i>c</i></b>	10100	1840	11600	316000
<b><i>d</i></b>	850	31.7	127	445

\*Fits of the dilution data displayed in Supplementary Fig. 12 to the four-parameter logistic equation:  $y = d + (a - d) / (1 + (x/c)^b)$ , where y is absorbance at 450 nm, and x is the fractional sample dilution (with 1 corresponding to no dilution). Fits to each of the four sample sets appear as lines in the figure.

**Supplementary Table 10. Differences in insulin receptor phosphorylation**

<i>Parameter*</i>	<i>PTP1B<sub>PS**</sub></i> <i>(light) Curve</i>	<i>Reference</i> <i>Curve</i>	<i>Average</i>	<i>SD</i>
<i>PTP1B<sub>PS**</sub> (light)/</i> <i>PTP1B<sub>PS**</sub> (light)</i>	1	N/A	N/A	N/A
<i>PTP1B<sub>PS**</sub> (light)/</i> <i>PTP1B<sub>PS**</sub> (dark)</i>	28.4	24.1	26.3	3.1
<i>Insulin (10 nM)/</i> <i>PTP1B<sub>PS**</sub> (light)</i>	4.3	3.1	3.3	0.5
<i>BBR (300 μM)/</i> <i>PTP1B<sub>PS**</sub> (light)</i>	3.7	2.9	3.7	0.8

\*We used the fits described in Supplementary Table 9 to estimate the fold-difference in concentration of phosphorylated insulin receptor between two samples: (i) PTP1B<sub>PS\*\*</sub>-expressing HEK293T/17 cells exposed to 455 nm light and (ii) a second sample. In the first column, we based these estimates on the dilution curve for the first sample; in the second column, we based them on the dilution curve of the second sample. Consistency between the two estimates suggests that they provide good quantitative metrics (See Supplementary Note 2).

## Supplementary References

1. Wu, Y. I. *et al.* A genetically encoded photoactivatable Rac controls the motility of living cells. *Nature* **461**, 104–108 (2009).
2. Buckley, A. M., Petersen, J., Roe, A. J., Douce, G. R. & Christie, J. M. LOV-based reporters for fluorescence imaging. *Curr. Opin. Chem. Biol.* **27**, 39–45 (2015).
3. Choy, M. S. *et al.* Conformational Rigidity and Protein Dynamics at Distinct Timescales Regulate PTP1B Activity and Allostery. *Mol. Cell* **65**, 644–658 (2017).
4. Karpinski, K. F. Optimality Assessment in the Enzyme-Linked Immunosorbent Assay (ELISA). *Biometrics* **46**, 381-390 (1990).
5. Nummer, S. A. *et al.* Updating the ELISA standard curve fitting process to reduce uncertainty in estimated microcystin concentrations. *MethodsX* **5**, 304-311 (2018).
6. Rowland, A. A., Chitwood, P. J., Phillips, M. J. & Voeltz, G. K. ER contact sites define the position and timing of endosome fission. *Cell* **159**, 1027–1041 (2014).
7. Tao, J., Malbon, C. C. & Wang, H. Y. Insulin Stimulates Tyrosine Phosphorylation and Inactivation of Protein-tyrosine Phosphatase 1B in Vivo. *J. Biol. Chem.* **276**, 29520–29525 (2001).
8. Cortesio, C. L. *et al.* Calpain 2 and PTP1B function in a novel pathway with Src to regulate invadopodia dynamics and breast cancer cell invasion. *J. Cell Biol.* **180**, 957–971 (2008).
9. Liu, F. & Chernoff, J. Protein tyrosine phosphatase 1B interacts with and is tyrosine phosphorylated by the epidermal growth factor receptor. *Biochem. J.* **327**, 139–145 (2015).

10. Dadke, S. *et al.* Regulation of protein tyrosine phosphatase 1B by sumoylation. *Nat. Cell Biol.* **9**, 80–85 (2007).
11. Gehrig, S. *et al.* An engineered photoswitchable mammalian pyruvate kinase. *FEBS J.* **284**, 2955–2980 (2017).
12. Dagliyan, O. *et al.* Engineering extrinsic disorder to control protein activity in living cells. *Science.* **354**, 1441–1444 (2016).
13. Yi, J. J., Wang, H., Vilela, M., Danuser, G. & Hahn, K. M. Manipulation of endogenous kinase activity in living cells using photoswitchable inhibitory peptides. *ACS Synth. Biol.* **3**, 788–795 (2014).
14. Yumerefendi, H. *et al.* Light-induced nuclear export reveals rapid dynamics of epigenetic modifications. *Nat. Chem. Biol.* **12**, 399–401 (2016).
15. Strickland, D. *et al.* TULIPs: Tunable, light-controlled interacting protein tags for cell biology. *Nat. Methods* **9**, 379–384 (2012).
16. Kaberniuk, A. A., Shemetov, A. A. & Verkhusha, V. V. A bacterial phytochrome-based optogenetic system controllable with near-infrared light. *Nat. Methods* **13**, 1–15 (2016).
17. Grusch, M. *et al.* Spatio-temporally precise activation of engineered receptor tyrosine kinases by light. *EMBO J.* **33**, 1713–1726 (2014).
18. Strickland, D., Moffat, K. & Sosnick, T. R. Light-activated DNA binding in a designed allosteric protein. *Proc. Natl. Acad. Sci.* **105**, 10709–10714 (2008).
19. Ryu, M.-H. *et al.* Engineering adenylate cyclases regulated by near-infrared window light. *Proc. Natl. Acad. Sci.* **111**, 10167–10172 (2014).
20. Richter, F. *et al.* Engineering of temperature- and light-switchable Cas9 variants. *Nucleic Acids Res.* **44**, 10003–10014 (2016).

21. Zhou, X. X., Fan, L. Z., Li, P., Shen, K. & Lin, M. Z. Optical control of cell signaling by single-chain photoswitchable kinases. *Science*. **355**, 836–842 (2017).
22. Bubeck, F. *et al.* Engineered anti-CRISPR proteins for optogenetic control of CRISPR–Cas9. *Nat. Methods* **15**, 924–927 (2018).
23. Lungu, O. I. *et al.* Designing Photoswitchable Peptides Using the AsLOV2 Domain. *Chem. Biol.* **19**, 507–517 (2012).
24. Taslimi, A. *et al.* Optimized second-generation CRY2-CIB dimerizers and photoactivatable Cre recombinase. *Nat. Chem. Biol.* **12**, 425–430 (2016).
25. Guntas, G. *et al.* Engineering an improved light-induced dimer (iLID) for controlling the localization and activity of signaling proteins. *Proc. Natl. Acad. Sci. U. S. A.* **112**, 112–117 (2015).
26. Wang, H. *et al.* LOVTRAP: An optogenetic system for photoinduced protein dissociation. *Nat. Methods* **13**, 755–758 (2016).